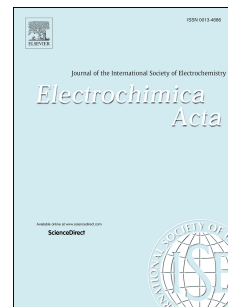# Accepted Manuscript

The role of molecular crowding in long-range metalloprotein electron transfer: Dissection into site- and scaffold-specific contributions

Ulises A. Zitare, Jonathan Szuster, Magali F. Scocozza, Andrés Espinoza-Cara, Alcides J. Leguto, Marcos N. Morgada, Alejandro J. Vila, Daniel H. Murgida

Please cite this article as: U.A. Zitare, J. Szuster, M.F. Scocozza, André. Espinoza-Cara, A.J. Leguto, M.N. Morgada, A.J. Vila, D.H. Murgida, The role of molecular crowding in long-range metalloprotein electron transfer: Dissection into site- and scaffold-specific contributions, *Electrochimica Acta* (2018), doi: https://doi.org/10.1016/j.electacta.2018.10.069.

1 The Role of Molecular Crowding in Long-Range Metalloprotein Electron Transfer:

2 Dissection into Site- and Scaffold-Specific Contributions

3

4 Ulises A. Zitare[a†], Jonathan Szuster[a†], Magali F. Scocozza[a], Andrés Espinoza-Cara[b], Alcides J.

5 Leguto[b], Marcos N. Morgada[b], Alejandro J. Vila[b], and Daniel H. Murgida[a*].

6

7 *a. Instituto de Química Física de los Materiales, Medio Ambiente y Energía (INQUIMAE),*

8 *Departamento de Química Inorgánica, Analítica y Química Física, Facultad de Ciencias*

9 *Exactas y Naturales, Universidad de Buenos Aires and CONICET,1428 Buenos Aires,*

10 *Argentina.*

11 *b. Instituto de Biología Molecular y Celular de Rosario (IBR), Departamento de Química*

12 *Biológica, Facultad de Ciencias Bioquímicas y Farmacéuticas, Universidad Nacional de*

13 *Rosario and CONICET, 2000 Rosario, Argentina.*

14 *† Equal contributions.*

15 ** Corresponding author. E-mail address: dhmurgida@qi.fcen.uba.ar*

16

17 Abstract

18 Here we report the effect of molecular crowding on long-range protein electron transfer

19 (ET) and disentangle the specific responses of the redox site and the protein milieu. To this

20 end, we studied two different one-electron redox proteins that share the cupredoxin fold

21 but differ in the metal centre, T1 mononuclear blue copper and binuclear Cu_A, and

22 generated chimeras with hybrid properties by incorporating different T1 centres within

the Cu_A scaffold or by swapping loops between orthologous proteins from different organisms to perturb the Cu_A site. The heterogeneous ET kinetics of the different proteins was studied by protein film electrochemistry at variable electronic couplings and in the presence of two different crowding agents. The results reveal a strong frictional control of the ET reactions, which for 10 Å tunnelling distances results in a 90% drop of the ET rate when viscosity is matched to that of the mitochondrial interior (ca. 55 cP) by addition of either crowding agent. The effect is ascribed to the dynamical coupling of the metal site and the milieu, which for T1 is found to be twice stronger than for Cu_A, and the activation energy of protein-solvent motion that is dictated by the overall scaffold. This work highlights the need of explicitly considering molecular crowding effects in protein ET.

Keywords

Metalloproteins, Loop Engineering, Electron Transfer, Molecular Crowding, Frictional Control.

1. Introduction

Most kinetic experimental studies of protein electron transfer (ET) reactions are performed with close to ideal diluted solutions[1–3] and rationalized within the framework of Marcus semiclassical equation for long-range (nonadiabatic) ET.[4,5] This treatment, implies a number of underlying assumptions that are not necessarily fulfilled for proteins in real biological environments,[6] which are characterized by high macromolecular crowding[7,8] and strong local electric fields.[9] For example, water-

1   protein nuclear fluctuations required to equalize donor-acceptor electronic energies

2   before ET, as well as the subsequent electrostatic relaxation, are assumed to be much

3   faster than electron tunnelling. This condition may break down due to either enhanced

4   electron tunnelling probability or to a slowdown (and eventually dynamical arrest) of

5   nuclear modes imposed by the milieu. Indeed, dynamical effects on ET reactions have

6   been theoretically addressed by a number of researchers such as Marcus,[10]

7   Weaver,[11] Zusman,[12] Jortner,[13] Beratan,[14] Waldeck,[15] Matyushov[16] and

8   others, employing different approximations. From the experimental side examples of

9   dynamical effects on protein ET reactions are rather limited and viscosity or crowding

10   studies on protein ET, although very valuable, mainly refer to the effect of crowding

11   agents on the diffusional component of interprotein ET in solution, rather than to the

12   electron tunnelling step.[17,18] Relevant to the present work, different authors studied

13   metalloproteins immobilized on electrodes coated with self-assembled monolayers

14   (SAMs) of functionalized alkanethiols, and found exponential distance-dependencies of

15   the measured ET rate constants (k_{ET}) only for thick SAMs, but distance-independent

16   plateaus for thinner spacers.[19–24] For the soluble metalloproteins cytochrome *c*[25–

17   27] and azurin[28–30] ET rates were found to be sensitive to the medium viscosity. These

18   observations were interpreted as a change of ET regime from nonadiabatic at longer

19   distances to frictional control in terms of Zusman´s equations at thinner

20   films,[25,26,28,29] and to electric field dependent protein-solvent collective motions of

21   large and small amplitude.[31–33] These preceding investigations demonstrate that

22   moderate viscosities may have an impact on long range ET rates. The goal of the present

1   work is to deepen our understanding of possible kinetic effects of biological molecular

2   crowding on protein ET and, more specifically, to dissect the contributions to this outcome

3   of the different structural and dynamical elements of metalloproteins that are relevant to

4   the ET reaction coordinate. To the best of our knowledge, this crucial issue remains to

5   date elusive and largely unexplored.

6   In this context it is pertinent to highlight the structural and dynamical complexity of

7   proteins, which requires multidimensional and hierarchical free energy landscapes to

8   describe the conformational substates explored at biologically relevant temperatures.

9   Time scales for such exploration are also hierarchical, ranging from femtoseconds for

10 bond vibrations, picoseconds to nanoseconds for side-chain rotations and microseconds

11 to seconds for collective motions of larger protein domains.[34] This flexibility at different

12 levels proved pivotal for canonical and alternative functions of different proteins and

13 enzymes.[35–43]

14   Based on notions adopted from the physical chemistry of glasses, Frauenfelder and

15 coworkers[44–46] formulated a model that divides protein fluctuations into three types:

16 α and β_h and vibrations. The α motions are associated to changes in the protein shape

17 and, therefore, are slaved to bulk solvent fluctuations, while β_h fluctuations refer to

18 internal protein motions and are slaved to the hydration shell. Hence, the surrounding

19 milieu (solvent) crucially assists protein function through structural and dynamical

20 modulation.[47,48] One should note, however, that the in vivo milieu seriously departs

21 from the nearly ideal behaviour of dilute aqueous solutions typically used for in vitro and

22 in silico studies. Cells present a number of large structures such as membranes and

1   cytoskeleton, as well as dissolved macromolecules in concentrations that can be as high as

2   450 g/L and occupy up to 40% of the cytoplasmic volume, in addition to a large variety of

3   small molecules.[7] In these complex and highly crowded environments fundamental

4   physicochemical parameters, such as viscosity, diffusion and activity coefficients, may

5   diverge from ideality by several orders of magnitude.[49–52] Moreover, crowding is

6   expected to reshape the free energy landscapes of proteins and, therefore, their

7   dynamics.[53] This may be particularly true for proteins that partake in respiratory

8   electron transfer (ET) chains of all living organisms. In eukariotes respiratory complexes

9   are embedded into the inner mitochondrial membrane (IM), while electron shuttles such

10   as cytochrome c are present at millimolar levels in the intermembrane space

11   (IMS).[41,54] These species coexist with about 49 other proteins present in the IMS and

12   481 proteins that are either integral or peripherally bound to the IM.[55] Moreover,

13   membrane-integral respiratory complexes may form giant supercomplexes (respirosomes)

14   of variable stoichiometry.[56,57] Such level of crowding undoubtedly affects the structure

15   and dynamics of water and, severally, those of the proteins themselves, as documented

16   for instance for small peptides and large photosynthetic complexes.[58–60]

17   The intricate electrostatic description of media such as the IM and the IMS adds

18   another layer of complexity. The IM is essentially an energy-transduction device that uses

19   a cascade of downhill ET reactions to drive proton translocation, thus building up a

20   gradient that energizes ATP synthesis. This proton gradient generates a transmembrane

21   potential that combined with the membrane surface and dipolar potentials may create

22   local electric fields of up to 0.1 V Å^{-1},[9] in addition to local contributions due to protein

1   surface charges. Experimental and theoretical investigations on model systems show that

2   electric fields of biologically meaningful magnitude may affect hydration, structure,

3   dynamics and reactivity of proteins,[61–64] as well as relaxation times, viscosity,

4   hydrogen bonding and other features of water.[65–72] Conceptually similar

5   considerations stand for other biological systems based on protein ET, such as in

6   photosynthesis and bacterial respiration.

7   As pointed out by Ellis[8] almost two decades ago, the potential of macromolecular

8   crowding to affect reactivity is obvious but often underappreciated, also for ET reactions.

9   In the present work, we specifically assess the role of frictional effects in protein ET, i.e.

10   of the viscosity component of molecular crowding. To this aim, we envisage an approach

11   that involves the engineering of different metal centers into two protein scaffolds.

12   Namely, we consider two different types of one-electron copper redox proteins that share

13   the cupredoxin fold but differ by their redox centers: the type 1 (T1) mononuclear blue

14   copper site and the purple binuclear Cu_A center. Protein samples with hybrid properties

15   were generated by loop engineering to obtain chimeras that incorporate different T1

16   centers within the Cu_A scaffold, as well as perturbed Cu_A sites obtained by loop

17   replacement without altering the protein scaffold.   The heterogeneous ET kinetics of the

18   different protein variants was studied by protein film electrochemistry at variable

19   electronic couplings and in the presence of two different crowding agents. The obtained

20   results reveal metal site- and scaffold-specific frictional control for tunnelling distances

21   shorter than ca. 24 Å.

22

1   **2. Experimental**

2   2.1 Protein preparation.

3   WT and mutant Cu_A-soluble fragments from subunit II of the cytochrome ba_3 from *T.*

4   *thermophilus* were produced as described previously[73–76] and stored in 100 mM

5   phosphate buffer (pH 6.0; 100 mM KCl). Azurin from Pseudomonas aeruginosa was

6   purchased from Sigma-Aldrich. Before use, protein samples were buffer exchanged to the

7   desired final condition by thorough filtration with Amicon Ultracel-5K filters employing a

8   refrigerated centrifuge at 4000 rpm and 4 °C (Hermile Z326K).

9

10   2.2 Protein film voltammetry.

11   Cyclic voltammetry (CV) experiments were performed with either a Gamry REF600 or a

12   PAR263A potentiostat using a water-jacketed non-isothermal cell. The cell was placed

13   inside a Faraday cage (Vista Shield) and equipped with a homemade polycrystalline gold

14   bead working electrode, a Pt wire auxiliary electrode and a Ag/AgCl (3 M KCl) reference

15   electrode. All potentials quoted here are referred to NHE. Prior to use Au electrodes were

16   oxidized in 10% $HClO_4$ applying a 3 V potential for 2 minutes, sonicated in 10% HCl for 15

17   minutes, rinsed with water and subsequently treated with a 1:3 v/v H_2O_2: H_2SO_4 mixture

18   at 120 °C. The electrodes were then subjected to repetitive voltage cycling between -0.2

19   and 1.6 V in 10% $HClO_4$. After thorough rinsing with water and ethanol, Au electrodes

20   were coated with self-assembled monolayers (SAMs) by overnight incubation in ethanolic

21   solutions containing 2mM $HS-(CH_2)_n-CH_3$ and 3mM $HS-(CH_2)_n-CH_2OH$. Before protein

22   adsorption SAM-coated electrodes were routinely cycled at 0.1 V s^{-1} within the potential

7

1   window required for each protein in 10 mM acetate buffer, pH 4.6, containing 250 mM

2   KNO_3. Electrodes used for subsequent experiments were those that showed a well

3   behaved and stable capacitive response only, with currents lower than 5 nA measured at

4   0.1 V s^{-1} for n = 15 and lower than 300 nA measured at 10 V s^{-1} for n = 5. Effective areas of

5   the working electrodes were obtained by CV before SAM-coating using 20 mM $Fe(CN)_6^{3-/4-}$

6   in 0.25 M KNO_3 as redox probe. The obtained values ranged from 2.6 to 7.9 mm^2, with an

7   average value of 6 mm^2. The SAM-modified electrodes were finally incubated in 0.1 to 0.5

8   mM protein solutions during 2 hours for protein adsorption, and then transferred to the

9   electrochemical cell. Measurements were performed in 10 mM acetate buffer, pH 4.6,

10   containing 250 mM KNO_3. The solution viscosity was adjusted by dissolving variable

11   amounts of either sucrose or polyethylene glycol 4000 (PEG4000) in the same

12   buffer/electrolyte mixture, thus maintaining constant ionic strength throughout all the

13   experiments. The temperature of the jacketed cell was varied employing a coupled

14   circulation thermostat (Lauda Alpha RA8) and continuously monitored with a

15   thermocouple (Fluke 51 II). CVs were typically acquired at scan rates between 50 and 500

16   mV s^{-1} for the thicker SAMs, and 1 to 60 V s^{-1} for the thinner films. All the CVs display the

17   shape characteristic of surface-confined redox species and linear variations of the anodic

18   and cathodic currents with the scan rate. Protein films were quite stable for about 100

19   voltammetry cycles. For longer cycling we observe a small gradual loss of the CV signals

20   without changes in peak positions and FWHM, which suggest slow desorption of the

21   protein film. CV measurements used throughout this work correspond to stable signals.

22   Electrodes were replaced by freshly prepared ones as soon as a small a drop of intensity

1   was detected. Rate constants were obtained using Laviron's formalism,[77] and activation

2   parameters were estimated from Arrhenius plots in a temperature range from ca. 5 °C to

3   40 °C.

4   Control kinetic experiments were performed using Creager´s method[78] based on

5   alternating current voltammetry (ACV). ACVs were acquired in stepped mode every 20 mV

6   in a potential window of 0.5 V centred on the reduction potential of each sample using an

7   rms amplitude of 10 mV. The range of frequencies was 1 Hz to 100 kHz for SAMs with n =

8   3, 5 and 7, 0.3 Hz to 30 kHz for n = 10 and 0.03 Hz to 30 Hz for n = 15.

9   Uncompensated resistance was routinely determined using the optimized impedance

10   routine included in the Framework Data Adquisition Software from Gamry (Version 6.33).

11   For Au electrodes coated with SAMs with n = 6, i.e. the thinnest SAMs that employed for

12   investigating viscosity effects, Ru values were typically 10 Ω in the absence of thickening

13   agent and 20 Ω at 5 cP. After protein adsorption Ru slightly increases, reaching values of

14   up to 40 and 50 Ω for viscosities of 1 and 5 cP, respectively, for the highest protein surface

15   concentrations employed here of ca. 8 pmol cm^{-2}, which are attained with azurine. The

16   highest currents obtained in CV experiments that are used for subsequent quantitative

17   treatment were achieved for azurine films on SAMs with n = 6 and scan rates of 60 V s^{-1}.

18   These maximum currents were about 40 µA and independent of the addition of thickening

19   agents. Based on these numbers, we can establish an upper limit for ohmic losses that is 2

20   mV for the most demanding conditions employed here, and typically one order of

21   magnitude lower or less.

1   CV measurements of bulk protein solutions were performed using a home-made water

2   jacketed non-isothermal three electrode cell that requires ca. 40 µL samples with

3   concentrations around 100 µM (10 mM buffer acetate, pH 4.6, 250 mM KNO_3). Gold

4   working electrodes were coated with HS-$(CH_2)_6$-OH to prevent protein adsorption.

5

6   2.3 Spectroscopic determinations.

7   UV-vis absorption spectra were acquired at 25 °C with a Thermo Scientific Evolution

8   Array spectrophotometer employing 1 cm or 0.1 cm path length as required, placed into a

9   jacketed cell-holder for temperature control trough a circulation thermostat (Fisherbrand

10   FBC620). Raman spectra were acquired in backscattering geometry with 532 nm excitation

11   using a Dilor XY800 Raman microscope equipped with a CCD detector. Prior to

12   measurement ca. 10 µL protein samples were placed and frozen at 77 K in a Linkam THMS

13   300 thermostat. RR spectra were acquired at 0.5 cm^{-1} resolution. UV-vis and RR

14   determinations were performed in 10 mM acetate buffer, pH 4.6, containing 250 mM

15   KNO_3, with and without addition of crowding agent.

16

17   **3. Results and discussion**

18   The present work aims to gain a deeper understanding of molecular crowding effects on

19   long-range protein ET and, specifically, to dissect the responses of the redox site and the

20   protein milieu to viscous media. The proteins selected for this study are: (i) wild type

21   azurin (Azu WT) from P. aeruginosa as a prototypical mononuclear T1 blue copper protein,

22   (ii) the Cu_A-containing soluble domain of the ba_3 O_2-reductase from *T. thermophilus* (Tt-

1   Cu_A) as a prototypical binuclear purple copper protein and (iii) three chimeric proteins

2   constructed by loop engineering of Tt-Cu_A where the sequences of the three loops that

3   surround the metal site are replaced by those corresponding to other organisms to create

4   novel T1 and Cu_A variants (Figure 1). The structure and spectroscopy of the WT and

5   chimeric proteins has been reported elsewhere.[43,73–76,79,80] Remarkable features

6   relevant to the present work are: (i) Tt-Cu_A and WT Azu share the cupredoxin motif, but

7   with some differences that elicit a higher thermal stability in Tt-Cu_A;[80–83] (ii) Azu WT is

8   a canonical T1 blue copper center;[3,84] (iii) Tt-Cu_A is canonical Cu_A centers, while Tt-3L is

9   a slightly distorted Cu_A site that preserves the mixed valence character and the typical

10   purple colour;[43,75] (iv) Ami-Cu_A and Azu-Cu_A are distorted and greenish mononuclear

11   T1 sites.[76]

12   The heterogeneous ET reactions of the five protein variants were investigated by

13   protein film electrochemistry using Au electrodes coated with self-assembled monolayers

14   (SAMs) of $SH-(CH_2)_n-CH_3$ / $SH-(CH_2)_n-CH_2OH$ mixtures in 4/6 proportion and variable length

15   (n = 3, 5, 7, 10 and 15). Proteins were adsorbed on the SAM-coated electrodes and

16   measured at pH 4.6 in 10 mM acetate buffer containing 250 mM KNO_3.

17   This combination of coating and electrolyte composition was adopted from previous

18   reports, which demonstrate that these conditions optimize adsorption without altering

19   the redox copper centers.[20,73,74,79] Cyclic voltammetry (CV) experiments afford quasi

20   reversible responses in all cases (Figures S1 to S4) with FWHM values close to ideal that, in

21   average, yield charge transfer coefficients between 0.45 and 0.55. Moreover, the

22   reduction potentials are very similar to those obtained in solution under comparable

1 conditions (Table S1), thus confirming the integrity of the adsorbed proteins. Surface-

2 enhanced RR spectra of the SAM-coated electrodes recorded before and after protein

3 adsorption do not exhibit changes in the intensity ratio of the $\Delta\nu_{C-S}$ bands characteristic of

4 the *gauche* and *trans* conformations of the alkanethiols found at 634 and 702 cm^{-1},

5 respectively (data not shown). [85] The intensity ratio of the $\Delta\nu_{C-S}$ bands is a sensitive

6 marker of order in SAMs and, therefore, its invariance strongly suggests that the SAM-

7 protein interactions are relatively weak and non-perturbative, in agreement with the

8 preservation of the reduction potentials of the adsorbed proteins.   From the integration

9 of the voltammetric peaks we obtain protein coverages that are typically below 4 pmol

10 cm^{-2} for Azu WT and below 2 pmol cm^{-2} for the other proteins, which represent less than

11 1/3 and 1/6 of full coverage, respectively, as estimated using a crystallographic diameter

12 of 40 Å for both scaffolds.

13   Since Chidsey´s seminal work,[86] SAM-coated electrodes are broadly used for kinetic

14 studies because they allow the systematic variation of protein-electrode electronic

15 coupling through the chain length of the thiols. Hence, we measured the ET rate

16 constant, k_{ET}, for the different protein variants as a function of the SAM thickness

17 employing two different and independent experimental approaches: Laviron's

18 formalism[77] based on the peak separation of CVs obtained at variable scan rates and

19 Creager´s method[78] based on variable frequency ac voltammetry. Figures S5 and S6

20 show typical Laviron´s working curves and trumpet plots, respectively, while a

21 representative Creager´s plot is presented in Figure S7. The two methods yield almost

22 identical k_{ET} values with a nearly 1:1 correspondence (Figures S8 and S9).

1   The results are summarized in Figures 2 and S10, and are characterized by an

2   exponential distance dependence of k_{ET} at thicker SAMs (n ≥ 10) and a softer dependency

3   at thinner films that tends to a plateau. Qualitatively similar results have been reported by

4   other authors for Azu WT and Tt-CuA, although with slightly lower rate constants

5   ascribable to the different experimental conditions.[20,28,30,87–89] The long distance

6   exponential decay, with tunnelling decay factor β ≈ 1 per methylene group, is the

7   fingerprint of a nonadiabatic ET mechanism.[90] The softer variation at shorter distances,

8   on the other hand, suggests a change of regime associated to the stronger electronic

9   coupling.

10   Waldeck et. al. observed a similar distance dependence for cytochrome *c* coordinatively

11   bound to pyridinyl-terminated alkanethiols and for Azu WT adsorbed on hydrophobic

12   SAMs, and ascribed it to a friction-controlled ET mechanism at shorter distances.[25,26,91]

13   Under the working hypothesis that Waldeck´s proposal is correct, we reason out that the

14   construction of chimeras as those summarized in Figure 1 offer a unique opportunity to

15   advance for the first time in assessing and dissecting biologically relevant crowding effects

16   on the ET reaction coordinate at different levels of the hierarchical protein architecture

17   and dynamics. To this end, we first investigated the impact on the ET kinetics of adding

18   variable amounts of sucrose and PEG4000 (Figures 3, S11 and S12). These two chemicals

19   were selected because are commonly used as crowding agents in biological studies due to

20   their ability to emulate in-cell high viscosities while minimizing specific interactions.[8] The

21   concentrations of the crowding agents were adjusted to produce viscosities up to 4 cP, i.e.

22   a typical cytosolic value, and control experiments were performed up to 60 cP, which

1   correspond to the typical intramitochondrial viscosity.[90–92]

2   In all these experiments electrolyte and buffer composition were kept constant, thus

3   fixing the ionic strength at I = 250 mM that, as shown in Figure S13, is sufficiently high to

4   warrant I-independent k_{ET} values, even at high viscosities.

5   For all the protein variants we observe a drop of k_{ET} upon addition of either crowding

6   agent. When plotted against the solution viscosity η, we obtain a power law dependence

7   of the form $k_{ET} \propto \eta^{-\gamma}$ (Figure 3) which, for a given protein at a given SAM thickness, is

8   nearly identical for the two crowding agents, thus pointing out that the kinetic effect most

9   likely arises from the increase of the bulk viscosity rather than due to specific interactions

10   of sucrose and PEG4000 with the different components of the SAM/protein systems.

11   Similar results are obtained in control experiments with extended viscosity range of up to

12   ca. 60 cP (Figure S14).

13   It is important to point out that additions of large amounts of sucrose or PEG4000 do

14   not affect the active sites, as resonance Raman and electronic absorption spectra remain

15   unaffected for all the protein variants studied here (Figures S15 and S16). In agreement

16   with these observations, CV responses are not affected by the crowding agents aside from

17   the increased peak separations (Figures S11 and S12). Indeed, reduction potentials remain

18   largely constant over a broad concentration range of crowding agents, with only some

19   minor variations for some of the protein variants and no changes for the others (Figure

20   S17), which may reflect slightly different sensitivity to changes in the dielectric constant.

21   Note that the addition of both crowding agents not only rises the viscosity but also

22   decreases the static dielectric constant (ε_s) and increases the optical dielectric constant

1   (ε_{op}) of the solution, which results in a reduction of the Pekar factor $\varepsilon_{op}^{-1} - \varepsilon_s^{-1}$ (Figure

2   S18). In terms of classical Marcus theory this would imply lower outer sphere

3   reorganization energies and, therefore, slightly faster ET. The results shown in Figure 3

4   suggest that the accelerating effect of a lower Pekar factor is overcompensated by the

5   slowing down effect of the higher viscosity, thus pointing out to a friction-controlled ET

6   reaction.

7   Interestingly, ET rates are sensitive to the solution viscosity not only in the plateau

8   region of the k_{ET} vs distance curves but, essentially for all chain lengths with n < 15, which

9   approximately corresponds to tunnelling distances < 23 Å.[95] As shown in Figure 4 for two

10 representative examples, the γ factors exhibit a sigmoidal distance dependence that

11 denotes the interplay between through-SAM electron tunnelling times and friction-

12 controlled protein dynamics.

13   Note that at the sub-monolayer coverages employed here, k_{ET} and activation free

14 energy values are insensitive to protein surface concentration (Figure S19), thereby

15 confirming that the observed kinetic effects are ascribable to the external crowding agent.

16 For SAMs with n = 5, which roughly corresponds to tunnelling distances of ca 10 Å, we

17 observe a 30-45 % drop of k_{ET} at η= 4 cP, and more than 90% drop at 55 cP. Interestingly,

18 in-cell local microviscosities have been reported to vary between 1 to 400 cP,[92] with

19 values of around 35-63 cP in healthy mitochondria and one order of magnitude higher

20 values under apoptotic conditions.[93,94]

21   The ET rate is given by the product of two terms: a Franck–Condon factor, which

22 accounts for the probability of achieving donor-acceptor energetic degeneracy through

15

thermal fluctuations, and the electronic coupling, which decays exponentially with

distance and represents the probability of electron tunnelling between degenerate states.

Both terms may be affected by molecular crowding through the increased viscosity. As

discussed in detail by Matyushov and coworkers,[96,97] the first term is sensitive to the

ratio between the reactant-product relaxation time (τ_{relax}) and the reaction time (τ_r).

Marcus theory works under the assumption that $\tau_{relax} \ll \tau_r$, which may not be valid in

slowly relaxing media, thus leading to a reduced phase sub-space accessible to thermal

exploration within the reaction time scale. This may result in a decrease of the apparent

Gibbs energy barrier and reorganization energy with respect to the Marcus equilibrium

values. Moreover, Matyushov et. al.[98] concluded that for the electrochemical ET of

cytochrome *c* the pre-exponential term of the ET rate constant is not affected by solvent

dynamics. In this scenario, one should expect an increase of k_{ET} upon raising the solvent

viscosity, as a result of lowering the activation barrier. The experimental results obtained

for the copper proteins studied here show the opposite trend, which strongly suggests

that the system does not reach the limiting case of $\tau_{relax} \ll \tau_r$ but, instead, the reaction

proceeds in an intermediate regime where the viscosity effect is dominated by the pre-

exponential factor. These experimental conditions are better described by Zusman

equation for electrochemical reduction at zero overpotential of adsorbed species:[91,99]

$$k_{ET} = \left(\frac{\lambda}{\pi^3 \tau_s^2 k_B T} \right)^{1/2} \left(e^{-\frac{\lambda}{4k_B T}} \right) ln \left(\frac{\rho |H_{DA}|^2 \pi^3 k_B T}{\lambda \hbar} \right) \quad (1)$$

where λ is the classical reorganization energy, τ_s is the solvent relaxation time, k_B is

Boltzmann constant, H_{DA} is the electronic coupling matrix element, ρ is the density of

1   states at the electrode surface and ℏ is the reduced Planck constant. In a usual first order

2   approximation, τ_s can be expressed in terms of the longitudinal relaxation time τ_L and,

3   thus, as a function of the solvent viscosity η and molar volume V_m:

4    $$\tau_s = \frac{\varepsilon_s}{\varepsilon_{op}} \tau_L = \frac{\varepsilon_s}{\varepsilon_{op}} \frac{3\eta V_m}{RT} \qquad (2)$$

5   Assuming a simple Debye solvent model, the viscosity can be described in terms of

6   Andrade's empirical equation:

7    $$\eta = A\, exp\left(\frac{\Delta G_s^{\#}}{RT}\right) \qquad (3)$$

8   where A is an empirical pre-exponential parameter and $\Delta G_s^{\#}$ is the activation free energy

9   for the solvent viscous flow.

10   As proposed by Waldeck and co-workers, the empirical power law $k_{ET} \propto \eta^{-\gamma}$, together

11   with equations 1-3 leads to the following approximated expression for the electrochemical

12   ET rate constant at zero driving force:[25,26,91]

13    $$k_{ET} = \frac{\varepsilon_{op}}{3A^{\gamma}V_m\varepsilon_s}\sqrt{\frac{RT\lambda}{4\pi}}\, exp\left(-\frac{\Delta G_{ET}^{\#}+\gamma \Delta G_s^{\#}}{k_BT}\right) \qquad (4)$$

14   where $\Delta G_{ET}^{\#} = \lambda/4$ is the classical Marcus activation free energy for ET. This equation

15   predicts that for a friction-controlled ET reaction the overall apparent activation free

16   energy, $\Delta G_{app}^{\#}$, contains a first term that represents the intrinsic ET reorganization energy

17   of the system and a second term, $\gamma \Delta G_s^{\#}$, which accounts for the temperature dependence

18   of the medium relaxation dynamics. $\Delta G_{app}^{\#}$ can be estimated from the temperature

19   dependence of k_{ET}. Arrhenius and Eyring treatments of these data yield essentially

20   identical results, in agreement with previous observations for similar copper

21   proteins[20,74,87] that the entropic contribution is negligibly small and, therefore,

17

1    $\Delta G_{app}^{\#} \approx \Delta H_{app}^{\#}$. Arrhenius plots obtained in the absence of crowding agents for the five

2   protein variants adsorbed on SAMs with n = 5 and n = 15 are shown in Figure S20, and the

3   results are summarized in Table S1. Note that for all the protein variants k_{ET} is

4   independent of solvent viscosity when measured using the thickest SAM, i.e. $\gamma = 0$ for n =

5   15, hence we obtain $\Delta H_{app}^{\#} \approx \Delta G_{ET}^{\#} = \lambda/4$ in these cases. $\Delta G_{s}^{\#}$ values can then be

6   obtained by subtracting $\Delta G_{ET}^{\#}$ measured at the thickest SAM from the $\Delta G_{app}^{\#}$ values

7   measured with thin films in the absence of crowding agents, and dividing by the

8   corresponding γ factors obtained from viscosity experiments with the thin SAMs. The two

9   relevant frictional parameters γ and $\Delta G_{s}^{\#}$ obtained for SAMs with n = 5 are plotted in

10   Figure 5. Interestingly, the value of γ seems to be a property of the metal site, with an

11   average value of 0.54 for the different native and non-native T1 centers, and an average

12   value of 0.29 for Tt-Cu$_A$ and Tt-3L. $\Delta G_{s}^{\#}$, in contrast, seems to be a specific property of the

13   protein scaffold, with an average value of 0.037 eV for the Tt-Cu$_A$ fold independently of

14   the metal center incorporated, and a value of 0.120 eV for the native azurin fold.

15   The parameter γ is a measure of the degree of frictional control, i.e. of the influence of

16   solvent/protein relaxation on the ET rate.[25,26] It is also an empirical correction that

17   accounts for the distribution of relaxation times not contemplated in the Debye solvent

18   model.[13] Limiting values of 0 and 1 correspond to the fully nonadiabatic and adiabatic

19   regimes, respectively, while values in between denote an intermediate regime with

20   overdamped solvent/protein dynamics, which is consistent with the observed distance

21   dependence of γ (Figure 4). The site specificity of γ revealed in the present work suggests

22   a more distinct interpretation for this parameter as a measure of the dynamic coupling

between the redox metal site and the protein/solvent milieu. This observation is

consistent with the structural rigidity of the Cu_2S_2 diamond core in Cu_A sites, which

includes a Cu-Cu covalent bond, compared to the more easily distorted T1 sites.[84]

On the other hand, $\Delta G_s^{\#}$ is similar, within experimental error, for all the protein variants

that share the Tt-Cu_A fold, with an average value of 0.037 eV. This value rises to 0.120 eV

for Azu WT. While both types of proteins are characterized by a high rigidity that is

regarded crucial to ensure efficient ET,[80,81] the lower melting temperatures of T1

proteins and backbone mobility studies by NMR reveal lower rigidity compared to

Cu_A.[80,82,83] At first sight this suggests the counterintuitive idea that the activation

parameter $\Delta G_s^{\#}$ is higher for more flexible proteins, which is reinforced by the even larger

value reported in literature for the highly flexible cytochrome *c* (Figure 5).[26] Our

proposal is that $\Delta G_s^{\#}$ is not reporting on the overall protein flexibility. Instead, this

scaffold-specific parameter is a measure of the temperature-dependence of protein-

solvent motions that are relevant to the ET reaction coordinate.

Given that the long-range ET rates for the systems studied here are within a range of

ca. 1 to 8000 Hz (Figures 2 and S10), low frequency protein-solvent motions may be

critical for the ET reaction. Moreover, protein-solvent dynamics may be affected by local

electric fields at the SAM/protein interface,[61,100] which are similar in magnitude to those

estimated for biological membranes,[101,102] thus possibly increasing $\Delta G_s^{\#}$ under in vivo

conditions with respect to diluted protein solution.

4. Conclusions

1   The present results highlight the need of explicitly considering molecular crowding effects

2   in protein ET reactions. Highly crowded environments, such as the mitochondrial

3   intermembrane space, are characterized by microviscosities that are one to two orders of

4   magnitude higher than for diluted aqueous solutions, and by the presence of high local

5   electric fields imposed by the membrane potentials that may affect protein-solvent

6   dynamics. Under these conditions nuclear motions relevant to the ET reaction coordinate

7   are overdamped, thus breaking down some of the underlying assumptions of Marcus

8   theory, and leading to a friction-controlled mechanism for electron tunnelling distances

9   shorter than ca. 24 Å. The degree of frictional control is determined by two parameters: (i)

10 the frictional activation barrier, which we show to be specific for the protein scaffold, and

11 (ii) the dynamical coupling between the redox site and the surrounding protein-solvent

12 milieu, which reports on the electronic structure and the functional features of the

13 electron transfer site. The first and second parameters resemble Frauenfelder´s α and β_h

14 fluctuations,[44–46] respectively, whose characteristic time scales are modulated by the

15 local electric fields and by the high viscosity prevailing in biological electron-proton energy

16 transduction. Overall, our strategy allows a dissection of the effects that impact on ET

17 under crowding conditions, as well as it opens new possibilities of studying in detail the

18 impact of these empirical parameters in a central biological phenomenon under

19 physiological conditions.

20

21 **Acknowledgements**

3

Appendix A. Supplementary data

5   Supplementary data related to this article can be found athttps://doi.org/xxxxx

6

References

8   [1]   J.R. Winkler, H.B. Gray, Electron Flow through Metalloproteins, Chemical Reviews. 114
9   (2014) 3369–3380. doi:10.1021/cr4004715.
10 [2]   C.C. Moser, M.M. Sheehan, N.M. Ennist, G. Kodali, C. Bialas, M.T. Englander, B.M. Discher,
11   P.L. Dutton, De Novo Construction of Redox Active Proteins, in: Methods in Enzymology,
12   Elsevier, 2016: pp. 365–388. doi:10.1016/bs.mie.2016.05.048.
13 [3]   J. Liu, S. Chakraborty, P. Hosseinzadeh, Y. Yu, S. Tian, I. Petrik, A. Bhagi, Y. Lu,
14   Metalloproteins Containing Cytochrome, Iron–Sulfur, or Copper Redox Centers, Chem. Rev.
15   114 (2014) 4366–4469. doi:10.1021/cr400479b.
16 [4]   R.A. Marcus, On the Theory of Electron-Transfer Reactions. VI. Unified Treatment for
17   Homogeneous and Electrode Reactions, The Journal of Chemical Physics. 43 (1965) 679–
18   701. doi:10.1063/1.1696792.
19 [5]   R.A. Marcus, N. Sutin, Electron transfers in chemistry and biology, Biochimica et Biophysica
20   Acta (BBA) - Reviews on Bioenergetics. 811 (1985) 265–322. doi:10.1016/0304-
21   4173(85)90014-X.
22 [6]   A. De la Lande, F. Cailliez, D. Salahub, Electron Transfer Reaction in Enzymes: Vanilla Marcus
23   Theory and How to Fix Them If They Do., in: Simulating Enzyme Reactivity: Computational
24   Methods in Enzyme Catalysis, 2017: pp. 89–149.
25 [7]   R.J. Ellis, A.P. Minton, Join the crowd: Cell biology, Nature. 425 (2003) 27–28.
26   doi:10.1038/425027a.
27 [8]   R.J. Ellis, Macromolecular crowding: obvious but underappreciated, Trends in Biochemical
28   Sciences. 26 (2001) 597–604. doi:10.1016/S0968-0004(01)01938-7.
29 [9]   R.J. Clarke, The dipole potential of phospholipid membranes and methods for its detection,
30   Advances in Colloid and Interface Science. 89–90 (2001) 263–281. doi:10.1016/S0001-
31   8686(00)00061-0.
32 [10] H. Sumi, R.A. Marcus, Dynamical effects in electron transfer reactions, The Journal of
33   Chemical Physics. 84 (1986) 4894–4914. doi:10.1063/1.449978.
34 [11] M.J. Weaver, Dynamical solvent effects on activated electron-transfer reactions: principles,
35   pitfalls, and progress, Chemical Reviews. 92 (1992) 463–480. doi:10.1021/cr00011a006.
36 [12] L.D. Zusman, Dynamical Solvent Effects in Electron Transfer Reactions, Zeitschrift Für
37   Physikalische Chemie. 186 (1994) 1–29. doi:10.1524/zpch.1994.186.Part_1.001.
38 [13] I. Rips, J. Jortner, Dynamic solvent effects on outer-sphere electron transfer, The Journal of
39   Chemical Physics. 87 (1987) 2090–2104. doi:10.1063/1.453184.

[14] D.N. Beratan, C. Liu, A. Migliore, N.F. Polizzi, S.S. Skourtis, P. Zhang, Y. Zhang, Charge Transfer in Dynamical Biosystems, or The Treachery of (Static) Images, Accounts of Chemical Research. 48 (2015) 474–481. doi:10.1021/ar500271d.

[15] A.K. Mishra, D.H. Waldeck, A Unified Model for the Electrochemical Rate Constant That Incorporates Solvent Dynamics, The Journal of Physical Chemistry C. 113 (2009) 17904–17914. doi:10.1021/jp9052659.

[16] D.V. Matyushov, Protein electron transfer: is biology (thermo)dynamic?, Journal of Physics: Condensed Matter. 27 (2015) 473001. doi:10.1088/0953-8984/27/47/473001.

[17] M. Hervás, J.A. Navarro, Effect of crowding on the electron transfer process from plastocyanin and cytochrome c6 to photosystem I: a comparative study from cyanobacteria to green algae, Photosynthesis Research. 107 (2011) 279–286. doi:10.1007/s11120-011-9637-1.

[18] B.G. Schlarb-Ridley, H. Mi, W.D. Teale, V.S. Meyer, C.J. Howe, D.S. Bendall, Implications of the Effects of Viscosity, Macromolecular Crowding, and Temperature for the Transient Interaction between Cytochrome *f* and Plastocyanin from the Cyanobacterium *Phormidium laminosum*, Biochemistry. 44 (2005) 6232–6238. doi:10.1021/bi047322q.

[19] Q. Chi, J. Zhang, J.E.T. Andersen, J. Ulstrup, Ordered Assembly and Controlled Electron Transfer of the Blue Copper Protein Azurin at Gold (111) Single-Crystal Substrates, J. Phys. Chem. B. 105 (2001) 4669–4679. doi:10.1021/jp0105589.

[20] K. Fujita, N. Nakamura, H. Ohno, B.S. Leigh, K. Niki, H.B. Gray, J.H. Richards, Mimicking Protein–Protein Electron Transfer: Voltammetry of Pseudomonas aeruginosa Azurin and the Thermus thermophilus CuA Domain at ω-Derivatized Self-Assembled-Monolayer Gold Electrodes, J. Am. Chem. Soc. 126 (2004) 13954–13961. doi:10.1021/ja047875o.

[21] D.H. Murgida, P. Hildebrandt, The heterogeneous electron transfer of cytochrome c adsorbed on Ag electrodes coated with ω-carboxyl alkanethiols. A surface enhanced resonance Raman spectroscopic study, Journal of Molecular Structure. 565–566 (2001) 97–100. doi:10.1016/S0022-2860(00)00781-X.

[22] A. Kranich, H. Naumann, F.P. Molina-Heredia, H.J. Moore, T.R. Lee, S. Lecomte, L.R. De, P. Hildebrandt, D.H. Murgida, Gated electron transfer of cytochrome c6 at biomimetic interfaces: a time-resolved SERR study, Physical Chemistry Chemical Physics. 11 (2009) 7390–7397. doi:10.1039/b904434e.

[23] P. Zuo, T. Albrecht, P.D. Barker, D.H. Murgida, P. Hildebrandt, Interfacial redox processes of cytochrome b562, Physical Chemistry Chemical Physics. 11 (2009) 7430–7436. doi:10.1039/b904926f.

[24] D.A. Capdevila, W.A. Marmisollé, F.J. Williams, D.H. Murgida, Phosphate mediated adsorption and electron transfer of cytochrome c. A time-resolved SERR spectroelectrochemical study, Physical Chemistry Chemical Physics. 15 (2013) 5386–5394. doi:10.1039/c2cp42044a.

[25] J. Wei, H. Liu, D.E. Khoshtariya, H. Yamamoto, A. Dick, D.H. Waldeck, Electron-Transfer Dynamics of Cytochrome C: A Change in the Reaction Mechanism with Distance, Angewandte Chemie International Edition. 41 (2002) 4700–4703. doi:10.1002/anie.200290021.

[26] H. Yue, D. Khoshtariya, D.H. Waldeck, J. Grochol, P. Hildebrandt, D.H. Murgida, On the electron transfer mechanism between cytochrome c and metal electrodes. Evidence for dynamic control at short distances, Journal of Physical Chemistry B. 110 (2006) 19906–19913. doi:10.1021/jp0620670.

1   [27]   A. Avila, B.W. Gregory, K. Niki, T.M. Cotton, An Electrochemical Approach to Investigate
2   Gated Electron Transfer Using a Physiological Model System: Cytochrome *c* Immobilized on
3   Carboxylic Acid-Terminated Alkanethiol Self-Assembled Monolayers on Gold Electrodes,
4   The Journal of Physical Chemistry B. 104 (2000) 2759–2766. doi:10.1021/jp992591p.

5   [28]   D.E. Khoshtariya, T.D. Dolidze, M. Shushanyan, K.L. Davis, D.H. Waldeck, R. van Eldik,
6   Fundamental signatures of short- and long-range electron transfer for the blue copper
7   protein azurin at Au/SAM junctions, Proceedings of the National Academy of Sciences. 107
8   (2010) 2757–2762. doi:10.1073/pnas.0910837107.

9   [29]   D.E. Khoshtariya, T.D. Dolidze, T. Tretyakova, D.H. Waldeck, R. van Eldik, Electron transfer
10   with azurin at Au–SAM junctions in contact with a protic ionic melt: impact of glassy
11   dynamics, Physical Chemistry Chemical Physics. 15 (2013) 16515. doi:10.1039/c3cp51896e.

12   [30]   L.J.C. Jeuken, J.P. McEvoy, F.A. Armstrong, Insights into Gated Electron-Transfer Kinetics at
13   the Electrode–Protein Interface: A Square Wave Voltammetry Study of the Blue Copper
14   Protein Azurin, The Journal of Physical Chemistry B. 106 (2002) 2304–2313.
15   doi:10.1021/jp0134291.

16   [31]   H.K. Ly, M.A. Marti, D.F. Martin, D. Alvarez-Paggi, W. Meister, A. Kranich, I.M. Weidinger, P.
17   Hildebrandt, D.H. Murgida, Thermal fluctuations determine the electron-transfer rates of
18   cytochrome c in electrostatic and covalent complexes, ChemPhysChem. 11 (2010) 1225–
19   1235. doi:10.1002/cphc.200900966.

20   [32]   A. Kranich, H.K. Ly, P. Hildebrandt, D.H. Murgida, Direct observation of the gating step in
21   protein electron transfer: Electric-field-controlled protein dynamics, Journal of the
22   American Chemical Society. 130 (2008) 9844–9848. doi:10.1021/ja8016895.

23   [33]   D. Alvarez-Paggi, W. Meister, U. Kuhlmann, I. Weidinger, K. Tenger, L. Zimányi, G. Rákhely,
24   P. Hildebrandt, D.H. Murgida, Disentangling electron tunneling and protein dynamics of
25   cytochrome c through a rationally designed surface mutation, Journal of Physical Chemistry
26   B. 117 (2013) 6061–6068. doi:10.1021/jp400832m.

27   [34]   K. Henzler-Wildman, D. Kern, Dynamic personalities of proteins, Nature. 450 (2007) 964–
28   972. doi:10.1038/nature06522.

29   [35]   V.C. Nashine, S. Hammes-Schiffer, S.J. Benkovic, Coupled motions in enzyme catalysis,
30   Current Opinion in Chemical Biology. 14 (2010) 644–651. doi:10.1016/j.cbpa.2010.07.020.

31   [36]   G. Wei, W. Xi, R. Nussinov, B. Ma, Protein Ensembles: How Does Nature Harness
32   Thermodynamic Fluctuations for Life? The Diverse Functional Roles of Conformational
33   Ensembles in the Cell, Chemical Reviews. 116 (2016) 6516–6551.
34   doi:10.1021/acs.chemrev.5b00562.

35   [37]   X.J. Jordanides, M.J. Lang, X. Song, G.R. Fleming, Solvation Dynamics in Protein
36   Environments Studied by Photon Echo Spectroscopy, The Journal of Physical Chemistry B.
37   103 (1999) 7995–8005. doi:10.1021/jp9910993.

38   [38]   J.T. King, K.J. Kubarych, Site-Specific Coupling of Hydration Water and Protein Flexibility
39   Studied in Solution with Ultrafast 2D-IR Spectroscopy, Journal of the American Chemical
40   Society. 134 (2012) 18705–18712. doi:10.1021/ja307401r.

41   [39]   D. Laage, T. Elsaesser, J.T. Hynes, Water Dynamics in the Hydration Shells of Biomolecules,
42   Chemical Reviews. 117 (2017) 10694–10725. doi:10.1021/acs.chemrev.6b00765.

43   [40]   S. Lampa-Pastirk, W.F. Beck, Polar Solvation Dynamics in Zn(II)-Substituted Cytochrome *c* :
44   Diffusive Sampling of the Energy Landscape in the Hydrophobic Core and Solvent-Contact
45   Layer, The Journal of Physical Chemistry B. 108 (2004) 16288–16294.
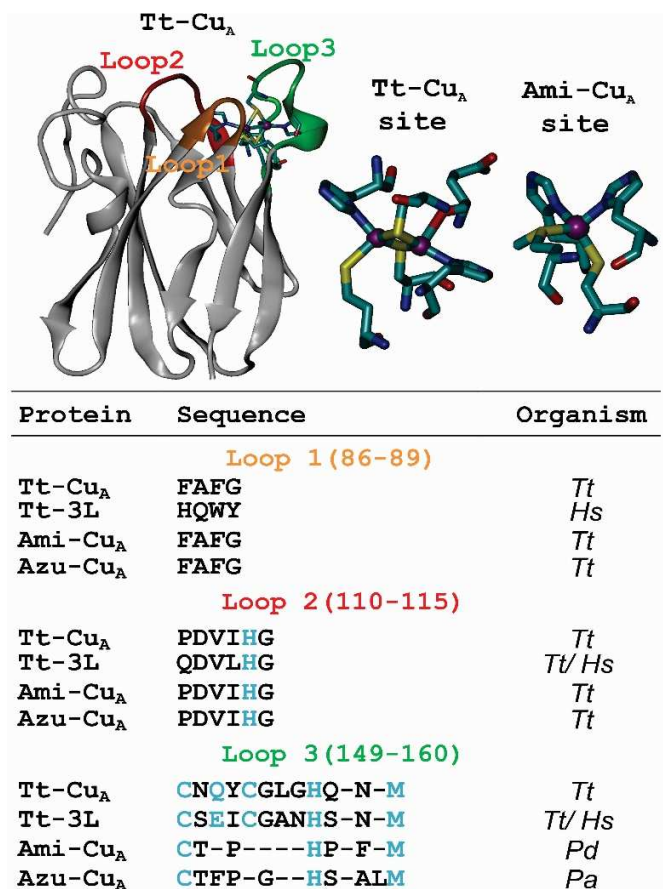46   doi:10.1021/jp0488113.

1 [41] D. Alvarez-Paggi, L. Hannibal, M.A. Castro, S. Oviedo-Rouco, V. Demicheli, V. Tórtora, F.
2   Tomasina, R. Radi, D.H. Murgida, Multifunctional Cytochrome c: Learning New Tricks from
3   an Old Dog, Chemical Reviews. 117 (2017) 13382–13460.
4   doi:10.1021/acs.chemrev.7b00257.
5 [42] L. Hannibal, F. Tomasina, D.A. Capdevila, V. Demicheli, V. Tórtora, D. Alvarez-Paggi, R.
6   Jemmerson, D.H. Murgida, R. Radi, Alternative Conformations of Cytochrome c: Structure,
7   Function, and Detection, Biochemistry. 55 (2016) 407–428.
8   doi:10.1021/acs.biochem.5b01385.
9 [43] D. Alvarez-Paggi, U.A. Zitare, J. Szuster, M.N. Morgada, A.J. Leguto, A.J. Vila, D.H. Murgida,
10   Tuning of Enthalpic/Entropic Parameters of a Protein Redox Center through Manipulation
11   of the Electronic Partition Function, Journal of the American Chemical Society. 139 (2017)
12   9803–9806. doi:10.1021/jacs.7b05199.
13 [44] H. Frauenfelder, S. Sligar, P. Wolynes, The energy landscapes and motions of proteins,
14   Science. 254 (1991) 1598–1603. doi:10.1126/science.1749933.
15 [45] H. Frauenfelder, G. Chen, J. Berendzen, P.W. Fenimore, H. Jansson, B.H. McMahon, I.R.
16   Stroe, J. Swenson, R.D. Young, A unified model of protein dynamics, PNAS. 106 (2009)
17   5129–5134. doi:10.1073/pnas.0900336106.
18 [46] P.W. Fenimore, H. Frauenfelder, S. Magazù, B.H. McMahon, F. Mezei, F. Migliardo, R.D.
19   Young, I. Stroe, Concepts and problems in protein dynamics, Chemical Physics. 424 (2013)
20   2–6. doi:10.1016/j.chemphys.2013.06.023.
21 [47] B.H. McMahon, H. Frauenfelder, P.W. Fenimore, The role of continuous and discrete water
22   structures in protein function, The European Physical Journal Special Topics. 223 (2014)
23   915–926. doi:10.1140/epjst/e2014-02125-y.
24 [48] M. C. Bellissent-Funel, A. Hassanali, M. Havenith, R. Henchman, P. Pohl, F. Sterpone, D. van
25   der Spoel, Y. Xu, A.E. Garcia, Water Determines the Structure and Dynamics of Proteins,
26   Chemical Reviews. 116 (2016) 7673–7697. doi:10.1021/acs.chemrev.5b00664.
27 [49] M. Gao, C. Held, S. Patra, L. Arns, G. Sadowski, R. Winter, Crowders and Cosolvents-Major
28   Contributors to the Cellular Milieu and Efficient Means to Counteract Environmental
29   Stresses, ChemPhysChem. 18 (2017) 2951–2972. doi:10.1002/cphc.201700762.
30 [50] J. van den Berg, A.J. Boersma, B. Poolman, Microorganisms maintain crowding homeostasis,
31   Nature Reviews Microbiology. 15 (2017) 309–318. doi:10.1038/nrmicro.2017.17.
32 [51] G. Rivas, A.P. Minton, Macromolecular Crowding In Vitro , In Vivo , and In Between, Trends
33   in Biochemical Sciences. 41 (2016) 970–981. doi:10.1016/j.tibs.2016.08.013.
34 [52] M.K. Kuimova, Mapping viscosity in cells using molecular rotors, Phys. Chem. Chem. Phys.
35   14 (2012) 12671–12686. doi:10.1039/C2CP41674C.
36 [53] M. Feig, I. Yu, P. Wang, G. Nawrocki, Y. Sugita, Crowding in Cellular Environments at an
37   Atomistic Level from Computer Simulations, The Journal of Physical Chemistry B. 121 (2017)
38   8009–8025. doi:10.1021/acs.jpcb.7b03570.
39 [54] J.M. Herrmann, J. Riemer, The Intermembrane Space of Mitochondria, Antioxidants &
40   Redox Signaling. 13 (2010) 1341–1358. doi:10.1089/ars.2009.3063.
41 [55] F.-N. Vögtle, J.M. Burkhart, H. Gonczarowska-Jorge, C. Kücükköse, A.A. Taskin, D.
42   Kopczynski, R. Ahrends, D. Mossmann, A. Sickmann, R.P. Zahedi, C. Meisinger, Landscape of
43   submitochondrial protein distribution, Nature Communications. 8 (2017).
44   doi:10.1038/s41467-017-00359-0.
45 [56] J. Gu, M. Wu, R. Guo, K. Yan, J. Lei, N. Gao, M. Yang, The architecture of the mammalian
46   respirasome, Nature. 537 (2016) 639–643. doi:10.1038/nature19359.

[57] R. Guo, S. Zong, M. Wu, J. Gu, M. Yang, Architecture of Human Mitochondrial Respiratory Megacomplex I 2 III 2 IV 2, Cell. 170 (2017) 1247-1257.e12. doi:10.1016/j.cell.2017.07.050.

[58] C. Lu, D. Prada-Gracia, F. Rao, Structure and dynamics of water in crowded environments slows down peptide conformational changes, The Journal of Chemical Physics. 141 (2014) 045101. doi:10.1063/1.4891465.

[59] R. Harada, Y. Sugita, M. Feig, Protein Crowding Affects Hydration Structure and Dynamics, Journal of the American Chemical Society. 134 (2012) 4842–4849. doi:10.1021/ja211115q.

[60] M. Malferrari, F. Francia, G. Venturoli, Retardation of Protein Dynamics by Trehalose in Dehydrated Systems of Photosynthetic Reaction Centers. Insights from Electron Transfer and Thermal Denaturation Kinetics, The Journal of Physical Chemistry B. 119 (2015) 13600–13618. doi:10.1021/acs.jpcb.5b02986.

[61] B. De, D.A. Paggi, F. Doctorovich, P. Hildebrandt, D.A. Estrin, D.H. Murgida, M.A. Marti, Molecular basis for the electric field modulation of cytochrome c structure and function, Journal of the American Chemical Society. 131 (2009) 16248–16256. doi:10.1021/ja906726n.

[62] I. Zoi, D. Antoniou, S.D. Schwartz, Electric Fields and Fast Protein Dynamics in Enzymes, The Journal of Physical Chemistry Letters. 8 (2017) 6165–6170. doi:10.1021/acs.jpclett.7b02989.

[63] S.D. Fried, S.G. Boxer, Electric Fields and Enzyme Catalysis, Annual Review of Biochemistry. 86 (2017) 387–415. doi:10.1146/annurev-biochem-061516-044432.

[64] P.K. Nandi, Z. Futera, N.J. English, Perturbation of hydration layer in solvated proteins by external electric and electromagnetic fields: Insights from non-equilibrium molecular dynamics, The Journal of Chemical Physics. 145 (2016) 205101. doi:10.1063/1.4967774.

[65] I. Danielewicz-Ferchmin, A.R. Ferchmin, Review: Water at ions, biomolecules and charged surfaces, Physics and Chemistry of Liquids. 42 (2004) 1–36. doi:10.1080/0031910031000120621.

[66] M. Druchok, M. Holovko, Structural changes in water exposed to electric fields: A molecular dynamics study, Journal of Molecular Liquids. 212 (2015) 969–975. doi:10.1016/j.molliq.2015.03.032.

[67] R. Richert, Relaxation time and excess entropy in viscous liquids: Electric field versus temperature as control parameter, The Journal of Chemical Physics. 146 (2017) 064501. doi:10.1063/1.4975389.

[68] C. Rønne, L. Thrane, P.O. Åstrand, A. Wallqvist, K.V. Mikkelsen, S.R. Keiding, Investigation of the temperature dependence of dielectric relaxation in liquid water by THz reflection spectroscopy and molecular dynamics simulation, The Journal of Chemical Physics. 107 (1997) 5319–5331. doi:10.1063/1.474242.

[69] A.M. Saitta, F. Saija, P.V. Giaquinta, *Ab Initio* Molecular Dynamics Study of Dissociation of Water under an Electric Field, Physical Review Letters. 108 (2012). doi:10.1103/PhysRevLett.108.207801.

[70] J. Sýkora, P. Kapusta, V. Fidler, M. Hof, On What Time Scale Does Solvent Relaxation in Phospholipid Bilayers Happen?, Langmuir. 18 (2002) 571–574. doi:10.1021/la011337x.

[71] A. Vegiri, Reorientational relaxation and rotational–translational coupling in water clusters in a d.c. external electric field, Journal of Molecular Liquids. 110 (2004) 155–168. doi:10.1016/j.molliq.2003.09.011.

[72] D. Zong, H. Hu, Y. Duan, Y. Sun, Viscosity of Water under Electric Field: Anisotropy Induced by Redistribution of Hydrogen Bonds, The Journal of Physical Chemistry B. 120 (2016) 4818–4827. doi:10.1021/acs.jpcb.6b01686.
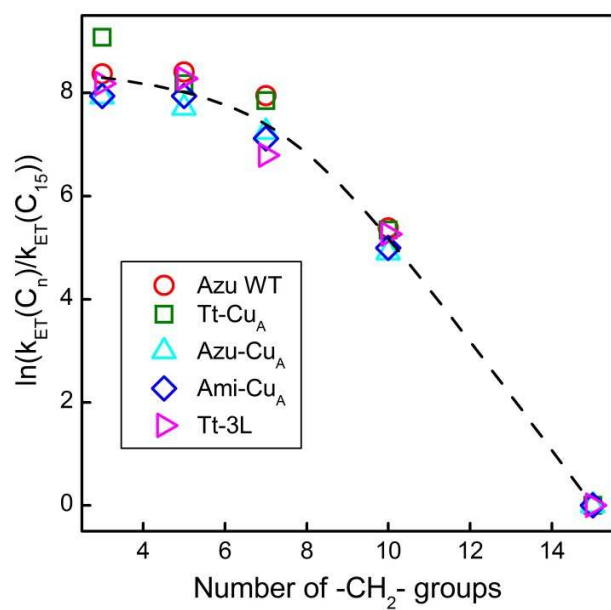
1   [73]   G.N. Ledesma, D.H. Murgida, K.L. Hoang, H. Wackerbarth, J. Ulstrup, A.J. Costa-Filho, A.J.
2   Vila, The met axial ligand determines the redox potential in CuA sites, Journal of the
3   American Chemical Society. 129 (2007) 11884–11885. doi:10.1021/ja0731221.

4   [74]   L.A. Abriata, D. Álvarez-Paggi, G.N. Ledesma, N.J. Blackburn, A.J. Vila, D.H. Murgida,
5   Alternative ground states enable pathway switching in biological electron transfer,
6   Proceedings of the National Academy of Sciences of the United States of America. 109
7   (2012) 17348–17353. doi:10.1073/pnas.1204251109.

8   [75]   M.N. Morgada, L.A. Abriata, U. Zitare, D. Alvarez-Paggi, D.H. Murgida, A.J. Vila, Control of
9   the electronic ground state on an electron-transfer copper site by second-sphere
10   perturbations, Angewandte Chemie - International Edition. 53 (2014) 6188–6192.
11   doi:10.1002/anie.201402083.

12   [76]   A. Espinoza-Cara, U.A. Zitare, D. Álvarez-Paggi, D.H. Murgida, A.J. Vila, Biosynthesis of Type
13   1 Copper Centers with Unusual Electronic and Functional Features by Loop Engineering,
14   Chem. Sci. 9 (2018) 6692-6702.

15   [77]   E. Laviron, General expression of the linear potential sweep voltammogram in the case of
16   diffusionless electrochemical systems, Journal of Electroanalytical Chemistry and Interfacial
17   Electrochemistry. 101 (1979) 19–28. doi:10.1016/S0022-0728(79)80075-3.

18   [78]   S.E. Creager, T.T. Wooster, A New Way of Using ac Voltammetry To Study Redox Kinetics in
19   Electroactive Monolayers, Anal. Chem. 70 (1998) 4257–4263. doi:10.1021/ac980482l.

20   [79]   U. Zitare, D. Alvarez-Paggi, M.N. Morgada, L.A. Abriata, A.J. Vila, D.H. Murgida, Reversible
21   Switching of Redox-Active Molecular Orbitals and Electron Transfer Pathways in CuA Sites
22   of Cytochrome c Oxidase, Angewandte Chemie - International Edition. 54 (2015) 9555–
23   9559. doi:10.1002/anie.201504188.

24   [80]   M.E. Zaballa, L.A. Abriata, A. Donaire, A.J. Vila, Flexibility of the metal-binding region in apo-
25   cupredoxins, PNAS. 109 (2012) 9254–9259. doi:10.1073/pnas.1119460109.

26   [81]   S.A. Pérez-Henarejos, L.A. Alcaraz, A. Donaire, Blue Copper Proteins: A rigid machine for
27   efficient electron transfer, a flexible device for metal uptake, Archives of Biochemistry and
28   Biophysics. 584 (2015) 134–148. doi:10.1016/j.abb.2015.08.020.

29   [82]   J. Chaboy, S. Díaz-Moreno, I. Díaz-Moreno, M.A. De la Rosa, A. Díaz-Quintana, How the
30   Local Geometry of the Cu-Binding Site Determines the Thermal Stability of Blue Copper
31   Proteins, Chemistry & Biology. 18 (2011) 25–31. doi:10.1016/j.chembiol.2010.12.006.

32   [83]   P. Wittung-Stafshede, B.G. Malmström, D. Sanders, J.A. Fee, J.R. Winkler, H.B. Gray, Effect
33   of Redox State on the Folding Free Energy of a Thermostable Electron-Transfer
34   Metalloprotein: The Cu $_A$ Domain of Cytochrome Oxidase from *Thermus thermophilus* [†],
35   Biochemistry. 37 (1998) 3172–3177. doi:10.1021/bi972901z.

36   [84]   E.I. Solomon, R.G. Hadt, Recent advances in understanding blue copper proteins,
37   Coordination Chemistry Reviews. 255 (2011) 774–789. doi:10.1016/j.ccr.2010.12.008.

38   [85]   W.A. Marmisollé, D.A. Capdevila, L.L. De, F.J. Williams, D.H. Murgida, Self-assembled
39   monolayers of NH2-terminated thiolates: Order, pKa, and specific adsorption, Langmuir. 29
40   (2013) 5351–5359. doi:10.1021/la304730q.

41   [86]   C.E.D. Chidsey, Free Energy and Temperature Dependence of Electron Transfer at the
42   Metal-Electrolyte Interface, Science. 251 (1991) 919–922.
43   doi:10.1126/science.251.4996.919.

44   [87]   S. Monari, G. Battistuzzi, C.A. Bortolotti, S. Yanagisawa, K. Sato, C. Li, I. Salard, D. Kostrz, M.
45   Borsari, A. Ranieri, C. Dennison, M. Sola, Understanding the Mechanism of Short-Range
46   Electron Transfer Using an Immobilized Cupredoxin, J. Am. Chem. Soc. 134 (2012) 11848–
47   11851. doi:10.1021/ja303425b.

1 [88] K. Yokoyama, B.S. Leigh, Y. Sheng, K. Niki, N. Nakamura, H. Ohno, J.R. Winkler, H.B. Gray,
2   J.H. Richards, Electron tunneling through Pseudomonas aeruginosa azurins on SAM gold
3   electrodes, Inorganica Chimica Acta. 361 (2008) 1095–1099. doi:10.1016/j.ica.2007.08.022.
4 [89] Q. Chi, O. Farver, J. Ulstrup, Long-range protein electron transfer observed at the single-
5   molecule level: In situ mapping of redox-gated tunneling resonance, Proceedings of the
6   National Academy of Sciences. 102 (2005) 16203–16208. doi:10.1073/pnas.0508257102.
7 [90] D.H. Murgida, P. Hildebrandt, Redox and redox-coupled processes of heme proteins and
8   enzymes at electrochemical interfaces, Physical Chemistry Chemical Physics. 7 (2005) 3773–
9   3784. doi:10.1039/b507989f.
10 [91] D.E. Khoshtariya, T.D. Dolidze, L.D. Zusman, D.H. Waldeck, Observation of the Turnover
11   between the Solvent Friction (Overdamped) and Tunneling (Nonadiabatic) Charge-Transfer
12   Mechanisms for a Au/Fe(CN)63-/4- Electrode Process and Evidence for a Freezing Out of
13   the Marcus Barrier, J. Phys. Chem. A. 105 (2001) 1818–1829. doi:10.1021/jp0041095.
14 [92] T. Liu, X. Liu, D.R. Spring, X. Qian, J. Cui, Z. Xu, Quantitatively Mapping Cellular Viscosity with
15   Detailed Organelle Information via a Designed PET Fluorescent Probe, Scientific Reports. 4
16   (2014) 5418. doi:10.1038/srep05418.
17 [93] Z. Yang, Y. He, J.-H. Lee, N. Park, M. Suh, W.-S. Chae, J. Cao, X. Peng, H. Jung, C. Kang, J.S.
18   Kim, A Self-Calibrating Bipartite Viscosity Sensor for Mitochondria, J. Am. Chem. Soc. 135
19   (2013) 9181–9185. doi:10.1021/ja403851p.
20 [94] N. Jiang, J. Fan, S. Zhang, T. Wu, J. Wang, P. Gao, J. Qu, F. Zhou, X. Peng, Dual mode
21   monitoring probe for mitochondrial viscosity in single cell, Sensors and Actuators B:
22   Chemical. 190 (2014) 685–693. doi:10.1016/j.snb.2013.09.062.
23 [95] D.H. Murgida, P. Hildebrandt, Heterogeneous electron transfer of cytochrome c on coated
24   silver electrodes. Electric field effects on structure and redox potential, Journal of Physical
25   Chemistry B. 105 (2001) 1578–1586.
26 [96] D.V. Matyushov, Protein electron transfer: Dynamics and statistics, The Journal of Chemical
27   Physics. 139 (2013) 025102. doi:10.1063/1.4812788.
28 [97] D.V. Matyushov, M.D. Newton, Electrode reactions in slowly relaxing media, The Journal of
29   Chemical Physics. 147 (2017) 194506. doi:10.1063/1.5003022.
30 [98] S.S. Seyedi, M.M. Waskasi, D.V. Matyushov, Theory and Electrochemistry of Cytochrome c,
31   The Journal of Physical Chemistry B. 121 (2017) 4958–4967. doi:10.1021/acs.jpcb.7b00917.
32 [99] L.D. Zusman, Outer-sphere electron transfer reactions at an electrode, Chemical Physics.
33   112 (1987) 53–59. doi:10.1016/0301-0104(87)85021-8.
34 [100] L. Khoa, N. Wisitruangsakul, M. Sezer, J.J. Feng, A. Kranich, I.M. Weidinger, I. Zebger, D.H.
35   Murgida, P. Hildebrandt, Electric-field effects on the interfacial electron transfer and
36   protein dynamics of cytochrome c, Journal of Electroanalytical Chemistry. 660 (2011) 367–
37   376. doi:10.1016/j.jelechem.2010.12.020.
38 [101] R.J. Clarke, The dipole potential of phospholipid membranes and methods for its detection,
39   Advances in Colloid and Interface Science. 89–90 (2001) 263–281. doi:10.1016/S0001-
40   8686(00)00061-0.
41 [102] J.K. Staffa, L. Lorenz, M. Stolarski, D.H. Murgida, I. Zebger, T. Utesch, J. Kozuch, P.
42   Hildebrandt, Determination of the Local Electric Field at Au/SAM Interfaces Using the
43   Vibrational Stark Effect, Journal of Physical Chemistry C. 121 (2017) 22274–22285.
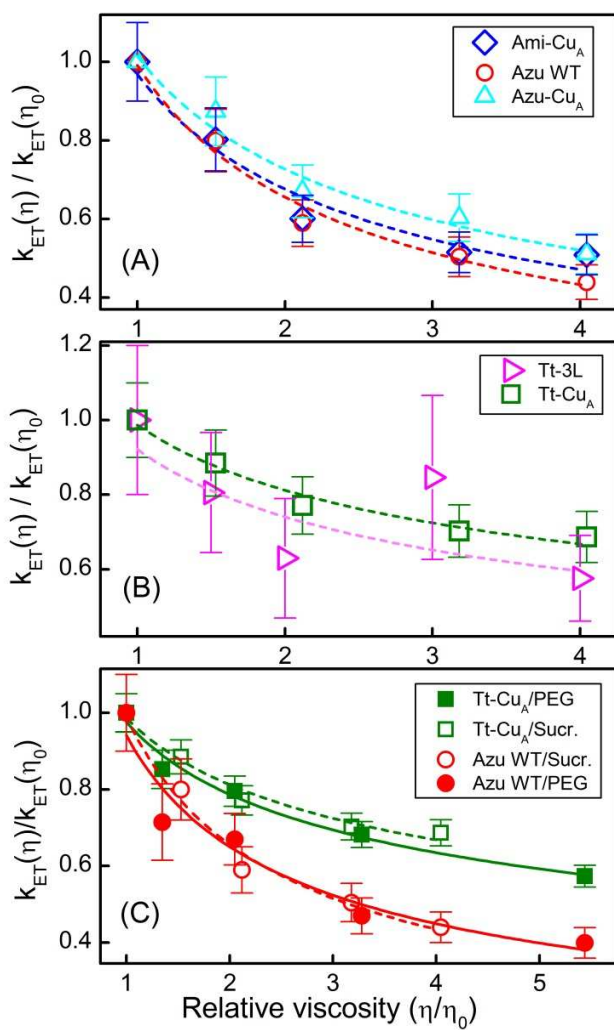44   doi:10.1021/acs.jpcc.7b08434.
45

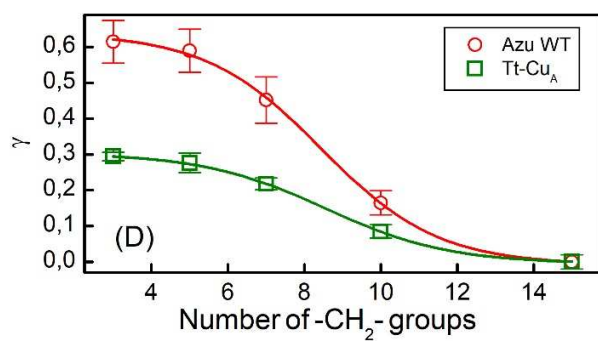| Protein	Sequence	Organism
	Loop 1(86-89)	
Tt-Cu$_A$	FAFG	Tt
Tt-3L	HQWY	Hs
Ami-Cu$_A$	FAFG	Tt
Azu-Cu$_A$	FAFG	Tt
	Loop 2(110-115)	
Tt-Cu$_A$	PDVIHG	Tt
Tt-3L	QDVLHG	Tt/Hs
Ami-Cu$_A$	PDVIHG	Tt
Azu-Cu$_A$	PDVIHG	Tt
	Loop 3(149-160)	
Tt-Cu$_A$	CNQYCGLGHQ-N-M	Tt
Tt-3L	CSEICGANHS-N-M	Tt/Hs
Ami-Cu$_A$	CT-P----HP-F-M	Pd
Azu-Cu$_A$	CTFP-G--HS-ALM	Pa

Figure 1.

1

2 **Figure 2.**

1

2   **Figure 3.**

3
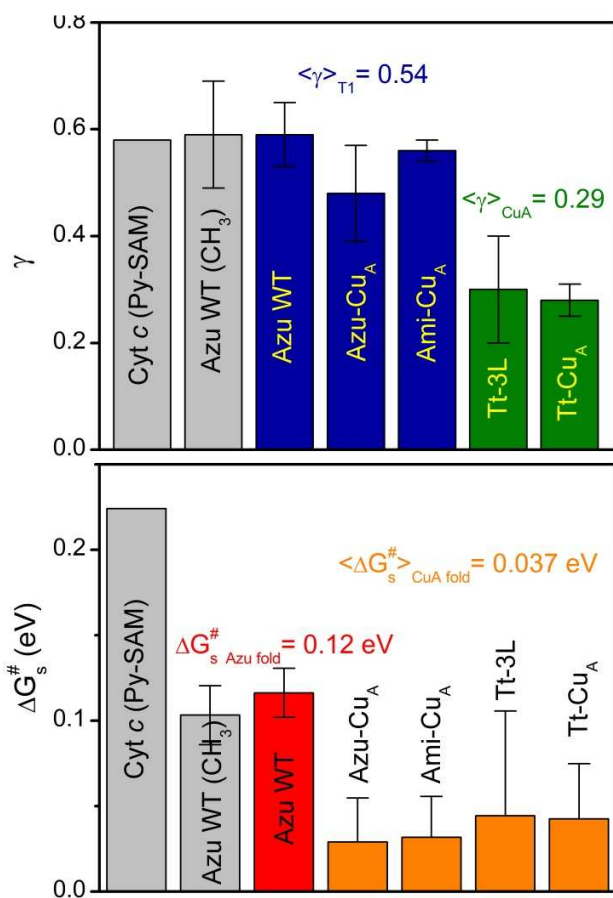
1

2   **Figure 4.**

3

Figure 5.

1   **Figure 1.** Top: Crystal structure of the Cu_A-containing soluble domain of the ba_3 O_2-

2   reductase from *Thermus thermophilus* (Tt-Cu_A; pdb 2CUA) and of the metal sites of the Tt-

3   Cu_A and Ami-Cu_A variants (pdb 2CUA and 5U7N, respectively). Bottom: sequences of the

4   three engineered loops. Letters in light blue denote first sphere ligands of the copper ions.

5   The last column indicates the organism from which the loop sequence was adopted for

6   the chimeras: Thermus thermophilus (Tt), Homo sapiens (Hs), Paracoccus denitrificans (Pc)

7   and Pseudomonas aeruginosa (Pa).

8

9   **Figure 2.** Normalized ET rate constants as a function of the SAM thickness. Each data point

10   is the average of at least three independent experiments performed at 25°C in 10 mM

11   acetate buffer, pH 4.6, containing 0.25 M KNO_3. Absolute k_{ET} values, as obtained by

12   Laviron´s method, are displayed in Figure S10.

13

14   **Figure 3.** Normalized ET rate constant as a function of the relative viscosity for proteins

15   adsorbed on SAMs with $n = 5$ (25°C; pH 4.6, 0.25 M KNO_3). (A) Monocuclear T1 centres.

16   (B) Binuclear Cu_A sites. (C) Comparison of Azu WT and Tt-Cu_A for experiments performed

17   with sucrose (empty symbols) or PEG4000 (filled symbols). The lines are fittings to

18   $k_{ET(\eta)} = k_{ET(\eta_0)}\eta^{-\gamma}$.

19

20   **Figure 4.** Frictional parameter γ as a function of SAM thickness for Azu WT and Tt-Cu_A

21   using sucrose as crowding agent. All measurements were performed at 25°C in 10 mM

22   acetate buffer (pH 4.6, 0.25 M KNO_3).

1   **Figure 5.** Empirical frictional parameter (γ) and activation free energy for the milleu

2   frictional motion ($\Delta G_s^{\#}$) for the copper proteins and wired Cyt c. Blue, green, red and

3   orange bars are data obtained in this work at 25°C in 10 mM acetate buffer (pH 4.6, 0.25

4   M KNO_3) and using $HS\text{-}(CH_2)_5\text{-}CH_3$/$HS\text{-}(CH_2)_5\text{-}$ CH_2OH SAMs. Gray bars are data taken from

5   literature for WT azurin on $HS\text{-}(CH_2)_5\text{-}CH_3$ SAMs (Azu WT (CH_3)) and cytochrome c

6   coordinated to a pyridinyl-terminated SAM (Cyt c (Py-SAM)).